




Cite this: *J. Mater. Chem. A*, 2019, 7, 2268

High-performance organic solar cells based on polymer donor/small molecule donor/nonfullerene acceptor ternary blends†

Shuixing Dai,^a Sreelakshmi Chandrabose,^b Jingming Xin,^c Tengfei Li,^a Kai Chen,^b Peiyao Xue,^a Kuan Liu,^a Ke Zhou,^c Wei Ma,^c Justin M. Hodgkiss^b and Xiaowei Zhan^a  [✉]

We used mid-bandgap small molecule donor TR as a third component to fabricate ternary nonfullerene organic solar cells (OSCs) based on narrow-bandgap polymer donor PTB7-Th and narrow-bandgap nonfullerene acceptor FOIC. TR exhibits full miscibility with PTB7-Th and efficient energy transfer to PTB7-Th, enhances stacking of PTB7-Th, hole mobility and charge generation of the blends, and ultimately improves device performance. Compared with the binary PTB7-Th/FOIC blend, the ternary device with 25% TR (w/w) yields simultaneously improved open-circuit voltage, short-circuit current density and fill factor. Finally, single-junction OSCs based on the ternary PTB7-Th/TR/FOIC blend yield power conversion efficiency as high as 13.1%, higher than the binary OSCs (12.1%). The ternary device efficiency exhibits high tolerance to thickness variation (>12% in the range of 80–200 nm). Transient absorption spectroscopy confirms the importance of long-range resonant energy transfer from donor to acceptor phases.

Received 3rd December 2018
Accepted 8th January 2019

DOI: 10.1039/c8ta11637g

rsc.li/materials-a

Introduction

Organic solar cells (OSCs) have been invented as a cost-effective solar energy conversion platform. Compared with traditional silicon-based solar cells, OSCs possess unique advantages, such as flexibility, lightweight, semitransparency and simple solution processing.^{1–3} Fullerene derivatives have been the widely used electron acceptors in the past two decades, and fullerene-based OSCs have achieved power conversion efficiencies (PCEs) over 11%.^{4–6} However, fullerene acceptors suffer from some drawbacks, such as limited chemical and electronic tunability, weak absorption in the visible and near-infrared (NIR) region and poor morphological stability, which imposes constraints on the further development of this field. In contrast, nonfullerene acceptors offer the possibility of addressing these deficiencies of fullerene acceptors.^{7–9} Recently, the development of nonfullerene acceptors has become a major focus of research.^{10–34} The conception and development of a class of nonfullerene

acceptors termed “fused-ring electron acceptor (FREA)”,^{17–27} particularly invention of the benchmark molecule ITIC,¹⁷ is advancing the OSCs field to a new level; now this field is shifting from fullerene to nonfullerene era.

Ternary blend strategy has been used to improve performance of the OSCs *via* absorption complementarity and energy-level modulation.^{35–46} For example, polymer donor/small molecule donor/PCBM ternary systems have been investigated, where introduction of small molecule donor into polymer/PCBM binary blend can tune the molecular orientation,³⁹ decrease π - π stacking distance and increase coherence length.³⁸ However, these fullerene-based ternary systems showed limited PCEs (generally <12%) due to the weak absorption of PCBM.^{38–41}

Here, we report the first example of ternary OSCs based on polymer donor/small molecule donor/nonfullerene acceptor, which exhibit a champion PCE > 13% and high tolerance to thickness variation (PCE > 12% in the range of 80–200 nm), and the first transient absorption study of a nonfullerene ternary blend. We previously reported a NIR-absorbing nonfullerene acceptor FOIC (Fig. 1a),⁴⁷ which exhibited a high PCE of 12%, when blended with a widely used narrow-bandgap polymer donor, PTB7-Th.⁴⁸ To enhance performance of this binary blend, a mid-bandgap small molecule donor TR⁴⁹ was introduced as a third component based on the following considerations: (1) both TR and PTB7-Th consist of alkylthio-thienyl-substituted benzo[1,2-*b*:4,5-*b'*] unit, which enables good compatibility when blended with each other. (2) absorption

^aDepartment of Materials Science and Engineering, College of Engineering, Key Laboratory of Polymer Chemistry and Physics of Ministry of Education, Peking University, Beijing 100871, China. E-mail: xwzhan@pku.edu.cn

^bMacDiarmid Institute for Advanced Materials and Nanotechnology, School of Chemical and Physical Sciences, Victoria University of Wellington, Wellington 6010, New Zealand

^cState Key Laboratory for Mechanical Behavior of Materials, Xi'an Jiaotong University, Xi'an 710049, China

† Electronic supplementary information (ESI) available. See DOI: 10.1039/c8ta11637g

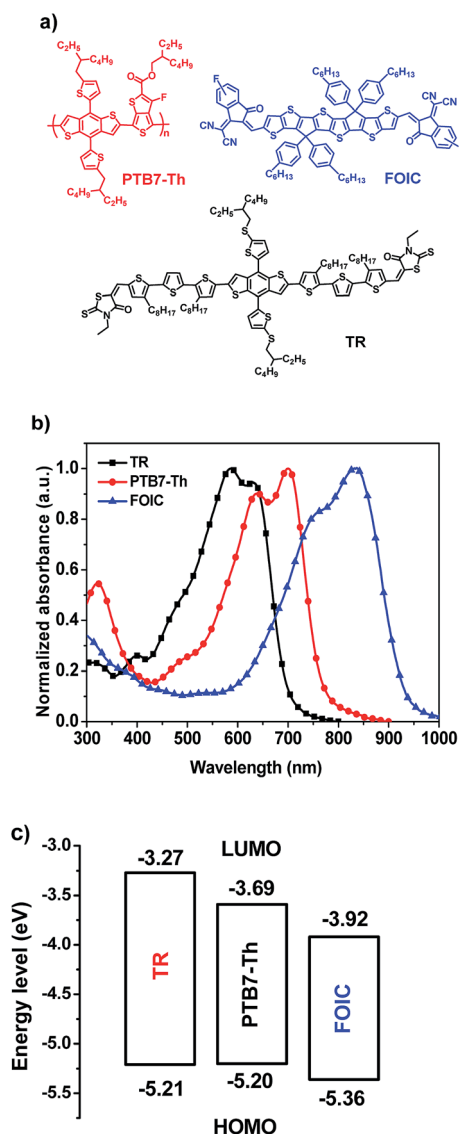


Fig. 1 (a) Chemical structures, (b) thin-film absorption spectra, and (c) energy levels of PTB7-Th, FOIC and TR.

spectrum of TR exhibits hypsochromic shift relative to that of PTB7-Th (Fig. 1b), which leads to panchromatic absorption of the blend. (3) The HOMO levels of donors TR and PTB7-Th are nearly aligned (Fig. 1c), ensuring that holes should be able to move freely between these materials without morphological trapping induced by the third component. (4) TR has high crystallinity and hole mobility ($3.2 \times 10^{-3} \text{ cm}^2 \text{ V}^{-1} \text{ s}^{-1}$),⁴⁹ which could enhance order and hole mobility of PTB7-Th *via* tuning the morphology of blended film. With this high-performance ternary system, we found that the third component TR plays an important role in modulating absorption profile and energy levels, enhancing molecular packing and hole mobility of the donor, and promoting energy transfer and charge generation. Transient absorption spectroscopy confirms the importance of long-range resonant energy transfer from donor to acceptor phases.

Results and discussion

Inverted devices with indium tin oxide (ITO)/ZnO/donor:FOIC/MoO_x/Ag were fabricated. The optimized PTB7-Th/FOIC weight ratio was 1 : 1.5,⁴⁷ the optimized additive diphenyl ether (DPE) content 0.5% (v/v) (Table S1, ESI†), and the optimized TR weight ratio 25% with respect to the donors (w/w) (Table S2, ESI†). The open-circuit voltage (V_{OC}) of OSCs increases from 0.722 V to 0.748 V as the TR weight ratio increases from 0 to 60% (Fig. S1, ESI†). The short-circuit current density (J_{SC}) and fill factor (FF) first increase then decrease as the TR weight ratio increases from 0 to 100%. When the TR weight ratio is 25%, the ternary devices yield the best PCE of 13.1%, with V_{OC} of 0.734 V, J_{SC} of 25.1 mA cm^{-2} and FF of 70.9% (Fig. 2a). After fabricating optimized ternary devices with active layer thickness from 80–300 nm (Table S3, ESI†), PCEs $\geq 12\%$ were found with thickness varying from 80 to 200 nm, and PCE = 10.8% with 300 nm thickness. This high tolerance to thickness variation indicates the promise of this ternary system for large-scale roll-to-roll printing.

The external quantum efficiency (EQE) spectra of the optimized devices are shown in Fig. 2b. PTB7-Th/FOIC binary blends exhibit higher EQEs in 450–900 nm, but weaker photoresponse below 450 nm. When incorporating TR, the ternary blends PTB7-Th/TR/FOIC exhibit enhanced EQE in 300–550 nm, but decreased photoresponse in 700–950 nm (Fig. S1b, ESI†). With increasing TR weight ratio, the absorption of blended film is enhanced in <550 nm region (Fig. S1c, ESI†), while decreased in 700–950 nm, which accounts for the trend in EQE. The J_{SC} values of the binary and ternary devices calculated from integration of the EQE spectra with the AM 1.5G reference spectrum are in good agreement with J_{SC} values measured from J - V (the error is <5%, Table S2, ESI†).

In order to understand the exciton generation, dissociation and charge extraction, we measured the photocurrent density (J_{ph}) versus the effective voltage (V_{eff}) of the OSCs (Fig. S2a, ESI†). J_{SC}/J_{sat} (saturation photocurrent density) characterizes the charge extraction under short-circuit condition. The J_{SC}/J_{sat} of optimized OSCs based on PTB7-Th/FOIC and PTB7-Th/TR/FOIC is 95.8% and 98.5%, respectively, indicating that the addition of TR in the ternary device further increases the charge dissociation and collection efficiency close to unity. Charge recombination was studied *via* measuring J_{SC} versus light density (P) (Fig. S2b, ESI†). The relationship between J_{SC} and P can be described as $J_{SC} \propto P^\alpha$.⁵⁰ The α values of PTB7-Th/FOIC and PTB7-Th/TR/FOIC-based OSCs are 0.96 and 0.97, respectively, suggesting negligible bimolecular charge recombination in both binary and ternary OSCs at short-circuit.

The SCLC method was used to measure the hole and electron mobilities of the blended films (Fig. S3, ESI†). The optimized ternary blend PTB7-Th/TR/FOIC exhibits a higher hole mobility ($6.8 \times 10^{-4} \text{ cm}^2 \text{ V}^{-1} \text{ s}^{-1}$) than PTB7-Th/FOIC ($4.0 \times 10^{-4} \text{ cm}^2 \text{ V}^{-1} \text{ s}^{-1}$) and TR/FOIC ($3.4 \times 10^{-4} \text{ cm}^2 \text{ V}^{-1} \text{ s}^{-1}$) parent binary blends. The electron mobility of PTB7-Th/TR/FOIC ($5.3 \times 10^{-4} \text{ cm}^2 \text{ V}^{-1} \text{ s}^{-1}$) is slightly higher than that of PTB7-Th/FOIC ($4.8 \times 10^{-4} \text{ cm}^2 \text{ V}^{-1} \text{ s}^{-1}$) but much higher than

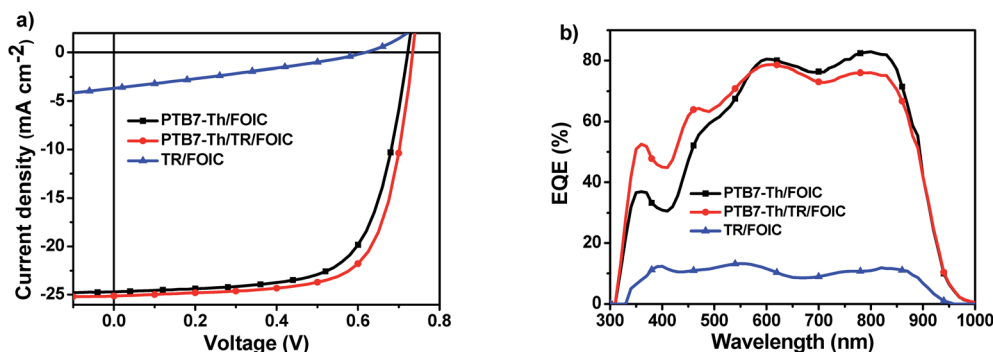


Fig. 2 (a) *J*-*V* characteristics and (b) EQE spectra of the best OSCs under illumination of an AM 1.5G at 100 mW cm⁻².

that of TR/FOIC (2.8×10^{-5} cm² V⁻¹ s⁻¹) (Table S4, ESI†). The higher charge mobilities are beneficial to the higher *J*_{SC} and higher FF of the ternary devices.

We used atomic force microscopy (AFM) to characterize the surface morphology of the binary and ternary blends (Fig. S4, ESI†). The root-mean-square (RMS) roughness of PTB7-Th/FOIC blend (3.52 nm) and TR/FOIC blend (2.83 nm) are larger than that of PTB7-Th/TR/FOIC (1.41 nm) ternary blend. Grazing-incidence wide-angle X-ray scattering (GIWAXS) measurements were carried out to probe the molecular packing information of these thin films.⁵¹ As shown in Fig. 3, the peaks located at 0.28 and 0.84 Å⁻¹ arise from the lamellar packing of PTB7-Th (the corresponding scattering of the neat films is shown in Fig. S5, ESI†). The peaks with *q* = 0.43, 0.86 and 1.29 Å⁻¹ originate from the lamellar packing of FOIC. The

lamellar packing peaks of TR are shown at *q* = 0.31, 0.62 and 0.93 Å⁻¹. The π-π stacking peaks of PTB7-Th, TR and FOIC are located at 1.58, 1.71 and 1.82 Å⁻¹, respectively. In Fig. 3, the lack of (010) peak (*q* = 1.58 Å⁻¹, Fig. S5, ESI†) of PTB7-Th both in PTB7-Th/TR and PTB7-Th/TR/FOIC blends proves two donors are totally miscible together. In the meantime, the (100) peak of PTB7-Th (*q* = 0.27 Å⁻¹) is sharper and coherence length increases from 5.0 to 7.5 nm, indicating that TR enhances the molecular packing of PTB7-Th, consistent with the increased hole mobility (Fig. S3a, ESI†).

Furthermore, resonant soft X-ray scattering (R-SoXS) was employed to characterize the phase separation of the blend films (Fig. 4).^{52,53} A photon energy of 284.2 eV was selected to maximize the materials contrast. The log-normal distributions exhibit a characteristic mode length scale $\xi_{\text{mode}} = 2\pi/q_{\text{mode}}$. The

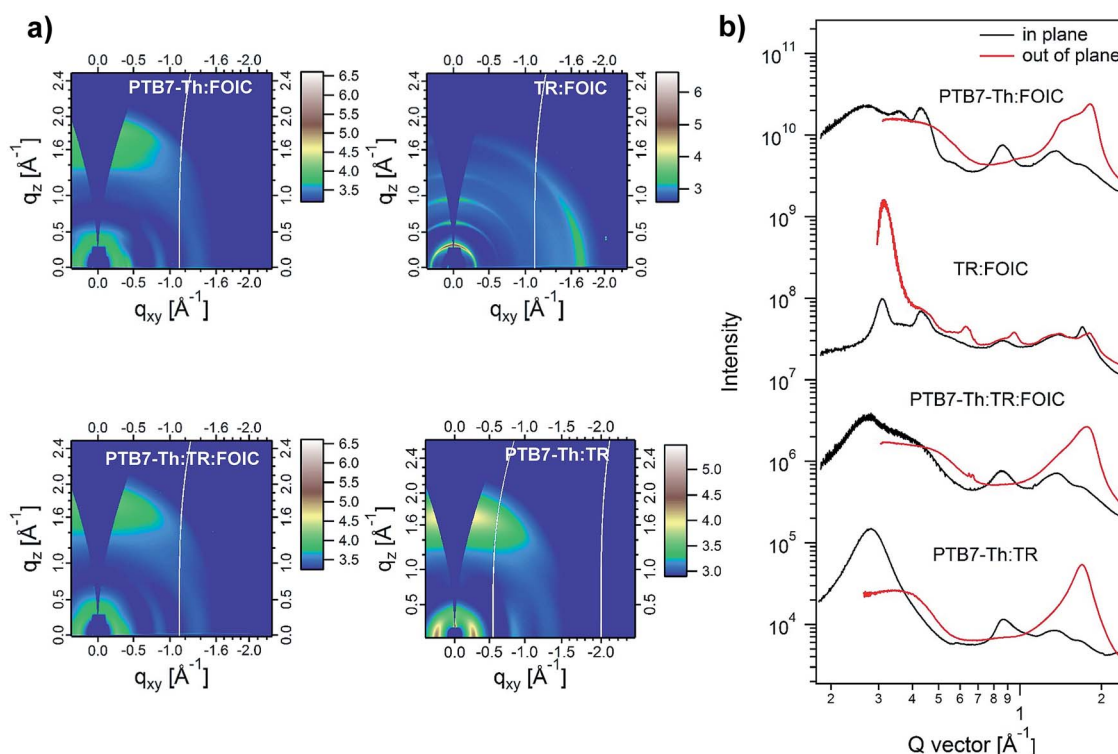


Fig. 3 GIWAXS 2D patterns (a) and 1D line-cuts (b) for optimized PTB7-Th/FOIC, TR/FOIC, PTB7-Th/TR/FOIC and PTB7-Th/TR blend films.

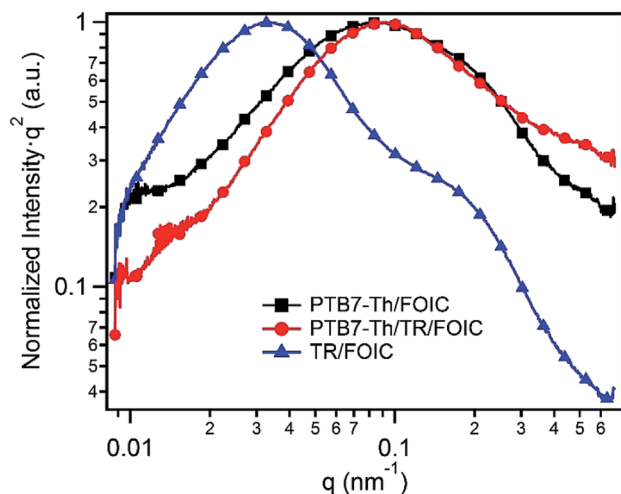


Fig. 4 R-SoXS profiles of optimized PTB7-Th/FOIC, TR/FOIC and PTB7-Th/TR/FOIC blend films.

mode domain size is half of ξ_{mode} . Both PTB7-Th/FOIC and TR/FOIC show two scattering peaks. The peaks at $\sim 0.2 \text{ nm}^{-1}$ originate from the surface roughness, which is confirmed by the scattering profiles at 270 eV (Fig. S6, ESI†). A large phase separation is observed in TR/FOIC blend film with the mode domain size of 97 nm, which is attributed to the high crystallinity of TR. Such large domain size limits the exciton dissociation, as confirmed in the photophysical measurements below. The mode domain size of PTB7-Th/FOIC is calculated to be 38 nm. The scattering profile of ternary system is similar to that of PTB7-Th/FOIC binary blend, also indicating good miscibility of PTB7-Th and TR.

The absorption spectrum of the PTB7-Th/TR/FOIC blend comprises contributions from each component (Fig. S7, ESI†), but linear decomposition of a binary PTB7-Th/TR blend absorption spectrum reveals that the presence of TR also strongly alters the PTB7-Th based spectrum. This spectral perturbation is also seen in photoluminescence (PL) spectra (Fig. S8, ESI†). In the PTB7-Th/TR blend, TR enhances the redder PL from PTB7-Th, but the PL peak from TR (expected *ca.* 715 nm) completely disappears, confirming that it is fully miscible with PTB7-Th.

Transient absorption (TA) spectroscopy for binary blends confirm that TR interacts strongly with PTB7-Th, but not with the FOIC acceptor. Upon exciting the PTB7-Th/TR blend at 500 nm, where both components absorb, sub-picosecond energy transfer occurs from TR to PTB7-Th, and the remaining spectrum of PTB7-Th excitons differs when TR is present (Fig. S9, ESI†). Moreover, the presence of TR decreases the exciton diffusion coefficient from $7.8 \times 10^{-3} \text{ cm}^2 \text{ s}^{-1}$ to $3.7 \times 10^{-3} \text{ cm}^2 \text{ s}^{-1}$, as ascertained by fluence dependent exciton annihilation measurements (Fig. S10, ESI†). The decreased diffusion coefficient in PTB7-Th is not expected to reduce the charge yield or hamper device performance in this case, since excitons are rapidly transferred to the FOIC phase (below). The underlying reasons for the decreased diffusion coefficient are beyond the scope of this study, perhaps relating to reduced

spectral overlap for resonant energy transfer, or to film morphology. In the FOIC/TR binary blend (Fig. S11, ESI†), the unperturbed and near-complete decay of the FOIC exciton signal (neat materials in Fig. S12, ESI†) and minimal remaining charge-based absorption confirms the R-SoXS finding that TR is not miscible with the FOIC phase.

TA spectroscopy was undertaken in the optimized ternary blend film to resolve the effect of TR on charge generation and recombination. The spectral series in Fig. 5a after 500 nm excitation reveals signatures of excitons in each phase on early timescales. In accordance with spectra of the neat materials,

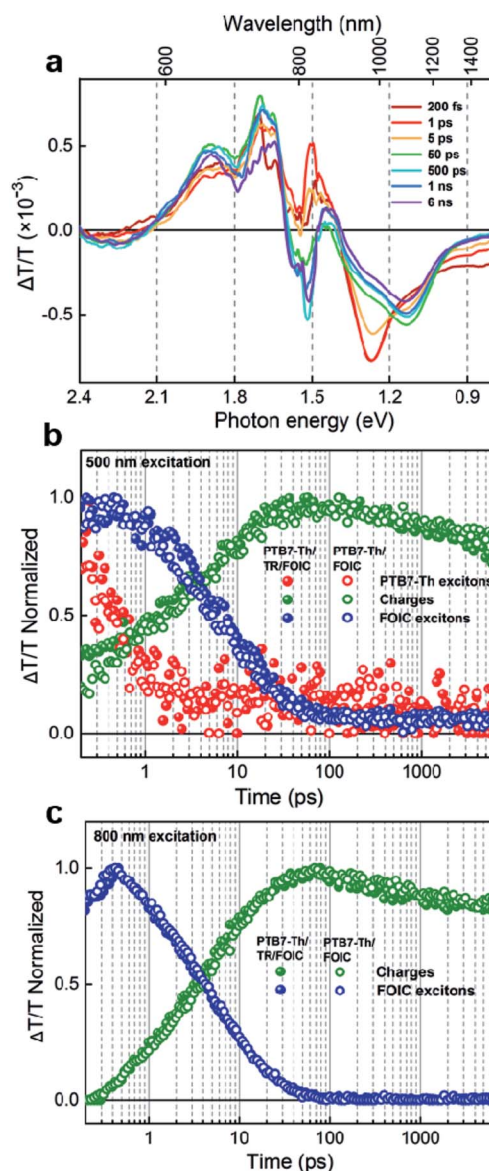


Fig. 5 (a) Series of transient absorption spectra for an optimized PTB7-Th/TR/FOIC ternary blend film after excitation at 500 nm ($0.9 \mu\text{J cm}^{-2}$), transient absorption kinetics of excitons and charges in the ternary (PTB7-Th/TR/FOIC) and the binary (PTB7-Th/FOIC) blends, excited at (b) 500 nm with pump fluences of $0.9 \mu\text{J cm}^{-2}$ and $0.8 \mu\text{J cm}^{-2}$, respectively and (c) 800 nm with pump fluences of $0.7 \mu\text{J cm}^{-2}$ and $0.6 \mu\text{J cm}^{-2}$, respectively.

FOIC excitons feature a photoinduced absorption (PIA) peak at 1.3 eV (Fig. S12a, ESI†) and PTB7-Th excitons are responsible for the PIA tail around 0.9 eV (Fig. S9, also ref. 54, along with the PTB7-Th/TR blend in Fig. S9, ESI†). TR-based exciton features (broad PIA around 1.1 eV, Fig. S12b, ESI†) are not clearly identifiable and may make a minor contribution on the sub-picosecond timescale, as per the binary PTB7-Th/TR blend. The absence of TR excitons beyond this ultrafast timescale confirms that TR is strongly intermixed with PTB7-Th, which is consistent with the GIWAXS data. The TA spectrum remaining on the nanosecond timescale in the optimized ternary blend can be attributed to charge pairs, retaining ground state bleach peaks from FOIC and PTB7-Th, complemented by charge-based photoinduced absorption from holes occupying PTB7-Th around 1100 nm (ref. 54) and electrons occupying FOIC presumed to account for the shoulder around 950 nm. This assignment is consistent with the TA spectra of binary blends shown in Fig. S11.† It is not possible to ascertain whether holes are also occupying TR in the ternary blend due to overlapping spectra with PTB7-Th.

Exciton-to-charge conversion dynamics for the optimized ternary blend and the PTB7-Th/FOIC binary blend are compared in Fig. 5b and c, with 500 nm and 800 nm excitation, respectively exciting the donor and acceptor phases. These plots are obtained *via* a bilinear decomposition of the TA surfaces using spectral masks of excitons and charges from the relevant neat and binary reference films (Fig. S11, S12, ESI†). Fig. 5b shows that, upon exciting the donor phase, PTB7-Th-based excitons are mostly quenched on the sub-picosecond timescale, but charges are formed on a slower ~ 10 picosecond timescale associated with the decay of FOIC excitons. The charge population peaks around 50 ps, beyond which non-geminate charge recombination sets in at the excitation densities used (confirmed *via* fluence dependent decay). The species-dependent kinetics confirm the importance of resonant energy transfer from donor to acceptor phases, as expected from absorption and PL spectra. The short lifetime of PTB7-Th-based excitons within pure phases exceeding 10 nm dimensions suggests that energy transfer operates over a long range. Similar dynamics are observed when exciting only the FOIC phase at 800 nm (Fig. 5c), but without the early contribution of PTB7-Th-based excitons and energy transfer (full spectral series in Fig. S13, ESI†). The low fraction of prompt charge generation with 500 nm excitation, and the lack of prompt charge generation with 800 nm excitation, confirms the high phase purity.

The spectral dynamics are remarkably similar for both PTB7-Th/TR/FOIC and PTB7-Th/FOIC blends. This similarity is expected based on the identical EQEs found at these excitation wavelengths (Fig. 2), and can be justified based on the slower exciton diffusion in PTB7-Th/TR/FOIC (Fig. S10, ESI†) being compensated by its enhanced red PL for resonant energy transfer into FOIC (Fig. S8, ESI†).

Conclusions

In summary, we used mid-bandgap small molecule donor TR as a third component to fabricate ternary nonfullerene OSC

devices based on narrow-bandgap polymer donor PTB7-Th and narrow-bandgap nonfullerene acceptor FOIC. When the TR weight ratio is 25% with respect to the donor component, the devices yield the best PCE of 13.1%, higher than the reference binary OSCs (12.1%). GIWAXS, R-SoXS and photophysics results confirm that TR is fully miscible with PTB7-Th but not miscible with FOIC. TR substantially alters the energy levels of PTB7-Th (as seen from the perturbed absorption and PL spectra), leading to higher V_{OC} in the ternary-blend OSCs relative to its binary counterpart. Both blends are found to benefit from rapid long-range resonant energy transfer from the electron donor (PTB7-Th) to electron acceptor (FOIC) phases. Enhanced stacking of PTB7-Th induced by high crystallinity of TR leads to increased hole mobility, which is beneficial to higher FF in the ternary blend.

Conflicts of interest

The authors declare no conflict of interest.

Acknowledgements

X. Z. wish to thank the NSFC (No. 21734001 and 51761165023). W. M. thanks for the support from Ministry of Science and Technology of China (No. 2016YFA0200700), NSFC (21504066, and 21704082). X-ray data was acquired at beamlines 7.3.3 and 11.0.1.2 at the Advanced Light Source, which is supported by the Director, Office of Science, Office of Basic Energy Sciences, of the U.S. Department of Energy under Contract No. DE-AC02-05CH11231. The authors thank Chenhui Zhu at beamline 7.3.3, and Cheng Wang at beamline 11.0.1.2 for assistance with data acquisition.

Notes and references

- 1 G. Li, W. H. Chang and Y. Yang, *Nat. Rev. Mater.*, 2017, **2**, 17043.
- 2 L. Lu, T. Zheng, Q. Wu, A. M. Schneider, D. Zhao and L. Yu, *Chem. Rev.*, 2015, **115**, 12666–12731.
- 3 F. C. Krebs, N. Espinosa, M. Hösel, R. R. Søndergaard and M. Jørgensen, *Adv. Mater.*, 2014, **26**, 29–39.
- 4 Z. C. He, B. Xiao, F. Liu, H. B. Wu, Y. L. Yang, S. Xiao, C. Wang, T. P. Russell and Y. Cao, *Nat. Photonics*, 2015, **9**, 174–179.
- 5 J. Zhao, Y. Li, G. Yang, K. Jiang, H. Lin, H. Ade, W. Ma and H. Yan, *Nat. Energy*, 2016, **1**, 15027.
- 6 M. Li, K. Gao, X. Wan, Q. Zhang, B. Kan, R. Xia, F. Liu, X. Yang, H. Feng, W. Ni, Y. Wang, J. Peng, H. Zhang, Z. Liang, H.-L. Yip, X. Peng, Y. Cao and Y. Chen, *Nat. Photonics*, 2017, **11**, 85–90.
- 7 Y. Lin and X. Zhan, *Acc. Chem. Res.*, 2016, **49**, 175–183.
- 8 C. Yan, S. Barlow, Z. Wang, H. Yan, A. K. Y. Jen, S. R. Marder and X. Zhan, *Nat. Rev. Mater.*, 2018, **3**, 18003.
- 9 P. Cheng, G. Li, X. Zhan and Y. Yang, *Nat. Photonics*, 2018, **12**, 131–142.

- 10 X. Zhan, Z. a. Tan, B. Domercq, Z. An, X. Zhang, S. Barlow, Y. Li, D. Zhu, B. Kippelen and S. R. Marder, *J. Am. Chem. Soc.*, 2007, **129**, 7246–7247.
- 11 P. E. Hartnett, A. Timalisina, H. S. Matte, N. Zhou, X. Guo, W. Zhao, A. Facchetti, R. P. Chang, M. C. Hersam, M. R. Wasielewski and T. J. Marks, *J. Am. Chem. Soc.*, 2014, **136**, 16345–16356.
- 12 Y. J. Hwang, H. Li, B. A. Courtright, S. Subramaniyan and S. A. Jenekhe, *Adv. Mater.*, 2016, **28**, 124–131.
- 13 Q. Wu, D. Zhao, A. M. Schneider, W. Chen and L. Yu, *J. Am. Chem. Soc.*, 2016, **138**, 7248–7251.
- 14 Y. Zhong, M. T. Trinh, R. Chen, G. E. Purdum, P. P. Khlyabich, M. Sezen, S. Oh, H. Zhu, B. Fowler, B. Zhang, W. Wang, C. Y. Nam, M. Y. Sfeir, C. T. Black, M. L. Steigerwald, Y. L. Loo, F. Ng, X. Y. Zhu and C. Nuckolls, *Nat. Commun.*, 2015, **6**, 8242.
- 15 D. Meng, H. Fu, C. Xiao, X. Meng, T. Winands, W. Ma, W. Wei, B. Fan, L. Huo, N. L. Doltsinis, Y. Li, Y. Sun and Z. Wang, *J. Am. Chem. Soc.*, 2016, **138**, 10184–10190.
- 16 J. Zhang, Y. Li, J. Huang, H. Hu, G. Zhang, T. Ma, P. C. Y. Chow, H. Ade, D. Pan and H. Yan, *J. Am. Chem. Soc.*, 2017, **139**, 16092–16095.
- 17 Y. Lin, J. Wang, Z.-G. Zhang, H. Bai, Y. Li, D. Zhu and X. Zhan, *Adv. Mater.*, 2015, **27**, 1170–1174.
- 18 Y. Lin, Q. He, F. Zhao, L. Huo, J. Mai, X. Lu, C. J. Su, T. Li, J. Wang, J. Zhu, Y. Sun, C. Wang and X. Zhan, *J. Am. Chem. Soc.*, 2016, **138**, 2973–2976.
- 19 Y. Lin, F. Zhao, Q. He, L. Huo, Y. Wu, T. C. Parker, W. Ma, Y. Sun, C. Wang, D. Zhu, A. J. Heeger, S. R. Marder and X. Zhan, *J. Am. Chem. Soc.*, 2016, **138**, 4955–4961.
- 20 S. Dai, F. Zhao, Q. Zhang, T. K. Lau, T. Li, K. Liu, Q. Ling, C. Wang, X. Lu, W. You and X. Zhan, *J. Am. Chem. Soc.*, 2017, **139**, 1336–1343.
- 21 Y. Lin, F. Zhao, Y. Wu, K. Chen, Y. Xia, G. Li, S. K. Prasad, J. Zhu, L. Huo, H. Bin, Z. G. Zhang, X. Guo, M. Zhang, Y. Sun, F. Gao, Z. Wei, W. Ma, C. Wang, J. Hodgkiss, Z. Bo, O. Inanias, Y. Li and X. Zhan, *Adv. Mater.*, 2017, **29**, 1604155.
- 22 F. Zhao, S. Dai, Y. Wu, Q. Zhang, J. Wang, L. Jiang, Q. Ling, Z. Wei, W. Ma, W. You, C. Wang and X. Zhan, *Adv. Mater.*, 2017, **29**, 1700144.
- 23 J. Wang, J. Zhang, Y. Xiao, T. Xiao, R. Zhu, C. Yan, Y. Fu, G. Lu, X. Lu, S. R. Marder and X. Zhan, *J. Am. Chem. Soc.*, 2018, **140**, 9140–9147.
- 24 W. Wang, C. Yan, T.-K. Lau, J. Wang, K. Liu, Y. Fan, X. Lu and X. Zhan, *Adv. Mater.*, 2017, **29**, 1701308.
- 25 J. Zhu, Z. Ke, Q. Zhang, J. Wang, S. Dai, Y. Wu, Y. Xu, Y. Lin, W. Ma, W. You and X. Zhan, *Adv. Mater.*, 2018, **30**, 1704713.
- 26 Y. Lin, F. Zhao, S. Prasad, J. Chen, W. Cai, Q. Zhang, K. Chen, Y. Wu, W. Ma, F. Gao, J. Tang, C. Wang, W. You, J. Hodgkiss and X. Zhan, *Adv. Mater.*, 2018, **30**, 1706363.
- 27 J. Wang, W. Wang, X. Wang, Y. Wu, Q. Zhang, C. Yan, W. Ma, W. You and X. Zhan, *Adv. Mater.*, 2017, **29**, 1702125.
- 28 Y. Yang, Z. G. Zhang, H. Bin, S. Chen, L. Gao, L. Xue, C. Yang and Y. Li, *J. Am. Chem. Soc.*, 2016, **138**, 15011–15018.
- 29 D. Baran, R. S. Ashraf, D. A. Hanifi, M. Abdelsamie, N. Gasparini, J. A. Rohr, S. Holliday, A. Wadsworth, S. Lockett, M. Neophytou, C. J. Emmott, J. Nelson, C. J. Brabec, A. Amassian, A. Salles, T. Kirchartz, J. R. Durrant and I. McCulloch, *Nat. Mater.*, 2017, **16**, 363–369.
- 30 Z. Fei, F. D. Eisner, X. Jiao, M. Azzouzi, J. A. Rohr, Y. Han, M. Shahid, A. S. R. Chesman, C. D. Easton, C. R. McNeill, T. D. Anthopoulos, J. Nelson and M. Heeney, *Adv. Mater.*, 2018, **30**, 1705209.
- 31 Y. Li, J. D. Lin, X. Che, Y. Qu, F. Liu, L. S. Liao and S. R. Forrest, *J. Am. Chem. Soc.*, 2017, **139**, 17114–17119.
- 32 S. Dai, T. Li, W. Wang, Y. Xiao, T. Lau, Z. Li, K. Liu, X. Lu and X. Zhan, *Adv. Mater.*, 2018, **30**, 1706571.
- 33 X. Che, Y. Li, Y. Qu and S. R. Forrest, *Nat. Energy*, 2018, **3**, 422–427.
- 34 S. Zhang, Y. Qin, J. Zhu and J. Hou, *Adv. Mater.*, 2018, **30**, 1800868.
- 35 P. Cheng and X. Zhan, *Mater. Horiz.*, 2015, **2**, 462–485.
- 36 L. Y. Lu, M. A. Kelly, W. You and L. P. Yu, *Nat. Photonics*, 2015, **9**, 491–500.
- 37 Y. Yang, W. Chen, L. T. Dou, W. H. Chang, H. S. Duan, B. Bob, G. Li and Y. Yang, *Nat. Photonics*, 2015, **9**, 190–198.
- 38 G. Zhang, K. Zhang, Q. Yin, X. F. Jiang, Z. Wang, J. Xin, W. Ma, H. Yan, F. Huang and Y. Cao, *J. Am. Chem. Soc.*, 2017, **139**, 2387–2395.
- 39 T. Kumari, S. M. Lee, S.-H. Kang, S. Chen and C. Yang, *Energy Environ. Sci.*, 2017, **10**, 258–265.
- 40 J. Zhang, Y. Zhang, J. Fang, K. Lu, Z. Wang, W. Ma and Z. Wei, *J. Am. Chem. Soc.*, 2015, **137**, 8176–8183.
- 41 P. Cheng, C. Yan, Y. Wu, J. Wang, M. Qin, Q. An, J. Cao, L. Huo, F. Zhang, L. Ding, Y. Sun, W. Ma and X. Zhan, *Adv. Mater.*, 2016, **28**, 8021.
- 42 H. Lu, J. Zhang, J. Chen, Q. Liu, X. Gong, S. Feng, X. Xu, W. Ma and Z. Bo, *Adv. Mater.*, 2016, **28**, 9559.
- 43 T. Liu, Y. Guo, Y. Yi, L. Huo, X. Xue, X. Sun, H. Fu, W. Xiong, D. Meng, Z. Wang, F. Liu, T. P. Russell and Y. Sun, *Adv. Mater.*, 2016, **28**, 10008.
- 44 P. Cheng, J. Wang, Q. Zhang, W. Huang, J. Zhu, R. Wang, S.-Y. Chang, P. Sun, L. Meng, H. Zhao, H.-W. Cheng, T. Huang, C. Wang, C. Zhu, W. You, X. Zhan and Y. Yang, *Adv. Mater.*, 2018, **30**, 1801501.
- 45 P. Cheng, R. Wang, J. Zhu, W. Huang, S.-Y. Chang, L. Meng, N. De Marco, P. Sun, H.-W. Cheng, J.-W. Lee, M. Qin, C. Zhu, X. Zhan and Y. Yang, *Adv. Mater.*, 2018, **30**, 1705243.
- 46 P. Cheng, M. Zhang, T.-K. Lau, Y. Wu, B. Jia, J. Wang, C. Yan, M. Qin, X. Lu and X. Zhan, *Adv. Mater.*, 2017, **29**, 1605216.
- 47 T. Li, S. Dai, Z. Ke, L. Yang, J. Wang, C. Yan, W. Ma and X. Zhan, *Adv. Mater.*, 2018, **30**, 1705969.
- 48 S.-H. Liao, H.-J. Jhuo, Y.-S. Cheng and S.-A. Chen, *Adv. Mater.*, 2013, **25**, 4766.
- 49 C. Cui, X. Guo, J. Min, B. Guo, X. Cheng, M. Zhang, C. J. Brabec and Y. Li, *Adv. Mater.*, 2015, **27**, 7469.
- 50 P. Schilinsky, C. Waldauf and C. J. Brabec, *Appl. Phys. Lett.*, 2002, **81**, 3885–3887.
- 51 A. Hexemer, W. Bras, J. Glossinger, E. Schaible, E. Gann, R. Kirian, A. MacDowell, M. Church, B. Rude and H. Padmore, *J. Phys.: Conf. Ser.*, 2010, **247**, 012007.

- 52 E. Gann, A. T. Young, B. A. Collins, H. Yan, J. Nasiatka, H. A. Padmore, H. Ade, A. Hexemer and C. Wang, *Rev. Sci. Instrum.*, 2012, **83**, 045110.
- 53 Y. Wu, Z. Y. Wang, X. Y. Meng and W. Ma, *Prog. Chem.*, 2017, **29**, 93–101.
- 54 K. D. Deshmukh, S. K. K. Prasad, N. Chandrasekaran, A. C. Y. Liu, E. Gann, L. Thomsen, D. Kabra, J. M. Hodgkiss and C. R. McNeill, *Chem. Mater.*, 2017, **29**, 804–816.